Alma Mater Studiorum, Bologna University
MSc in Aerospace Engineering

Project Report for the course:
Advanced Guidance and Control of Aircraft and Spacecraft

Adaptive Control of Helicopter Attitude in presence of Flapping Disturbances and Model Uncertainties

Student:
Francesco Sessini

To the attention of:
Prof. Paolo Castaldi

February 2025

Contents

1 Introduction

Helicopter flight dynamics are inherently complex due to the strong coupling between rotational and translational motions, as well as the significant influence of external disturbances such as wind gusts and rotor flapping. These factors make the design of robust control systems for helicopters particularly challenging. Traditional control strategies often rely on linearized models, which may not adequately capture the non-linearities and uncertainties present in real-world flight conditions. This project focuses on the development of an intelligent control system for helicopter attitude regulation, specifically addressing the challenges posed by flapping disturbances and model uncertainties.

The primary objective of this project is to design and implement a Feedback Error Learning (FEL) controller enhanced by a Radial Basis Function Neural Network (RBF-NN) for the attitude control of a teetering rotor helicopter. The FEL controller is chosen for its ability to combine the robustness of traditional feedback control with the adaptive capabilities of neural networks. The RBF-NN is employed to estimate and compensate for unmodeled dynamics and external disturbances, thereby improving the overall performance of the control system.

The helicopter model used in this study is a non-linear, 6-degree-of-freedom (6DoF) model based on the BELL AH-1 attack helicopter. The model incorporates the dynamics of the main rotor, tail rotor, and fuselage, as well as the effects of rotor flapping and fuselage drag. The control system is designed to regulate the helicopter's attitude by commanding cyclic and pedal inputs, with the RBF-NN providing online adaptation to account for uncertainties and disturbances.

This report is structured as follows: section 2 presents the helicopter model and the controller architecture, including the linearized model and the design of the FEL controller and of the RBF neural network. Section 3 discusses the simulation results, comparing the closed loop response of the controlled system using the linear and the non-linear model, and evaluating the controller's ability to track attitude setpoints and trajectories under wind shear conditions. Finally, section 4 sums up the conclusions and some future work possibilities.

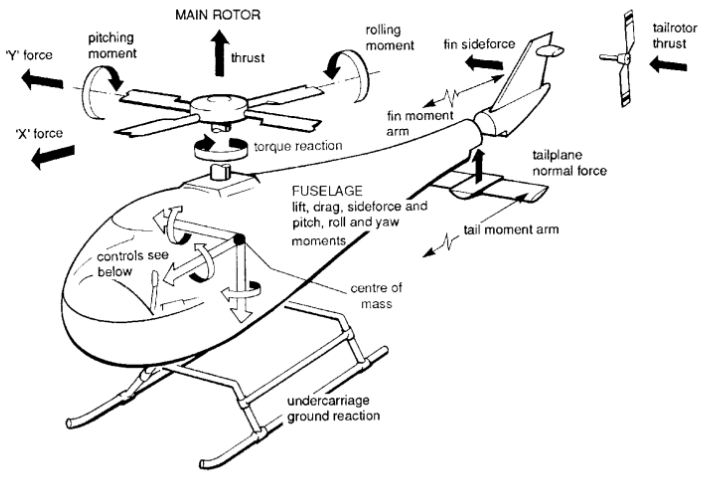

Figure 1: Schematic diagram of helicopter components.[4]

2 Helicopter model and controller architecture

In this project we will develop a Feedback Error Learning (FEL) controller architecture for the attitude control of a teetering rotor helicopter. The goal is to make the controller robust towards the model non-linearities and the external disturbances, which are represented by wind gusts that affect rotor flapping and the total drag of the vehicle. To this aim, the controller is enhanced by a Radial Basis Function Neural Network (RBF-NN) which, through on-line updating of its weighting matrix, predicts the uncertainty term in the control law.

A non-linear, 6 degree of freedom model for the dynamics of the teetering helicopter was developed and is presented in the following section. Then the design of the control law based on the linearized model is addressed, together with the RBF-NN structure.

2.1 Helicopter model

This section introduces the helicopter model and its dynamic characteristics. The helicopter's motion is governed by a set of nonlinear differential equations that describe the interaction between forces and moments generated by the main rotor, tail rotor and fuselage. The parameters used are from a BELL AH-1 attack helicopter and are listed in appendix A, with the corresponding variables nomenclature as used in the implementation.

2.1.1 Reference frames

Three right-handed orthogonal reference frames are introduced:

1. An Earth-fixed North-East-Down frame, $\mathcal{F}_E = \{O_E; x_E, y_E, z_E\}$: the origin, O_E, is arbitrarily fixed to a point on the Earth's surface, x_E aims in the direction of the geodetic North, z_E points downwards along the Earth's ellipsoid normal, and y_E completes a right-handed triad. This frame is assumed to be inertial under the assumption of a flat and non-rotating Earth.

2. A Local Vertical frame, $\mathcal{F}_V = \{CG; x_H, y_H, z_H\}$: the origin is located at the vehicle's center of gravity, CG. Under the hypothesis of a flat Earth, $\mathcal{F}_V$ has axes parallel to $\mathcal{F}_E$.

3. A body-fixed frame, $\mathcal{F}_B = \{CG; x_B, y_B, z_B\}$: the x_B-axis is positive out the nose of the rotorcraft in its plane of symmetry, z_B is perpendicular to x_B in the same plane of symmetry, pointing downwards, and y_B completes a right-handed triad and thus points to port.

4. A rotor hub-body frame $\mathcal{F}_{HB} = \{HUB; x_{HB}, y_{HB}, z_{HB}\}$, with axis parallel to $\mathcal{F}_B$, centered in the rotor hub.

5. A rotor hub-wind frame $\mathcal{F}_{HW} = \{HUB; x_{HW}, y_{HW}, z_{HW}\}$, with x_{HW} aligned with the relative wind direction in the plane of the rotor, centered in the rotor hub, with z_{HW} parallel to z_{HB}.

2.1.2 Equations of motion

The equations of motion for a helicopter are expressed in the body-fixed frame and include translational and rotational dynamics. The translational dynamics are described

by Newton's second law:

$$m\dot{\vec{v}}_B = -\vec{\omega} \times m\vec{v}_B + \vec{f} \tag{1}$$

where m is the helicopter's mass, $\vec{v}$ is the velocity vector, $\vec{\omega}$ is the angular velocity and $\vec{f}$ represents the aerodynamic, gravitational, and control forces. The rotational dynamics follow Euler's equations:

$$\underline{\underline{I}}\dot{\vec{\omega}} = -\vec{\omega} \times \underline{\underline{I}}\vec{\omega} + \vec{\tau} \tag{2}$$

where $\underline{\underline{I}}$ is the inertia matrix and $\vec{\tau}$ represents external moments. The angular rates are $\vec{\omega} = [p, q, r]$ and the Euler angles are defined by $\vec{\alpha} = [\phi, \theta, \psi]$. The positional and angular kinematics are given by:

$$\dot{p_E} = \underline{\underline{T}}^t_{bv} \cdot \vec{v}_B \tag{3}$$

$$\dot{\vec{\alpha}} = \underline{\underline{W}} \cdot \vec{\omega} \tag{4}$$

With the rotation matrices being:

$$\underline{\underline{T}}_{bv} = \begin{bmatrix} c\theta\, c\psi & c\theta\, s\psi & -s\theta \\ s\phi\, s\theta\, c\psi - c\phi\, s\psi & s\phi\, s\theta\, s\psi + c\phi\, c\psi & s\phi\, c\theta \\ c\phi\, s\theta\, c\psi + s\phi\, s\psi & c\phi\, s\theta\, s\psi - s\phi\, c\psi & c\phi\, c\theta \end{bmatrix} \tag{5}$$

$$\underline{\underline{W}} = \begin{bmatrix} 1 & s\phi\, t\theta & c\phi\, t\theta \\ 0 & c\phi & -s\phi \\ 0 & s\phi/c\theta & c\phi/c\theta \end{bmatrix} \tag{6}$$

The forces and moments acting on the helicopter center of gravity according to Godbolt[3] are:

$$\vec{f} = \begin{pmatrix} -T_M a_{1s} - H_x \\ T_M b_{1s} - T_T - H_y \\ -T_M \end{pmatrix} + \underline{\underline{T}}_{bv} \begin{pmatrix} 0 \\ 0 \\ g \end{pmatrix} \tag{7}$$

$$\vec{\tau} = \vec{l}_T \times \begin{pmatrix} 0 \\ -T_T \\ 0 \end{pmatrix} + \vec{l}_M \times \begin{pmatrix} -T_M a_{1s} - H_x \\ T_M b_{1s} - H_y \\ -T_M \end{pmatrix} + \begin{pmatrix} 0 \\ -Q_T \\ Q_M \end{pmatrix} \tag{8}$$

where T_M and T_T are the main rotor and tail rotor thrust, a_{1s} and b_{1s} are the first harmonic flapping angles w.r.t. the shaft in the main rotor hub-body frame, $\vec{l}_M$ and $\vec{l}_T$ are the coordinates vectors of main rotor and tail rotor in body axis (thus their moment arm w.r.t. the cg), Q_M and Q_T are the rotors torques, H is the main rotor drag commonly referred to as the *H-force*.

2.1.3 Main rotor and tail rotor

The derivation for thrust, drag and torque of the rotors is taken from Talbot.[6] Rotor inflow is considered uniform and calculated through the Glauert theory for forward flight with the formula:

$$\lambda = \frac{v_i}{\Omega R} = \frac{w_H}{\Omega R} - \frac{C_T}{2\sqrt{\mu^2 \lambda^2}} \tag{9}$$

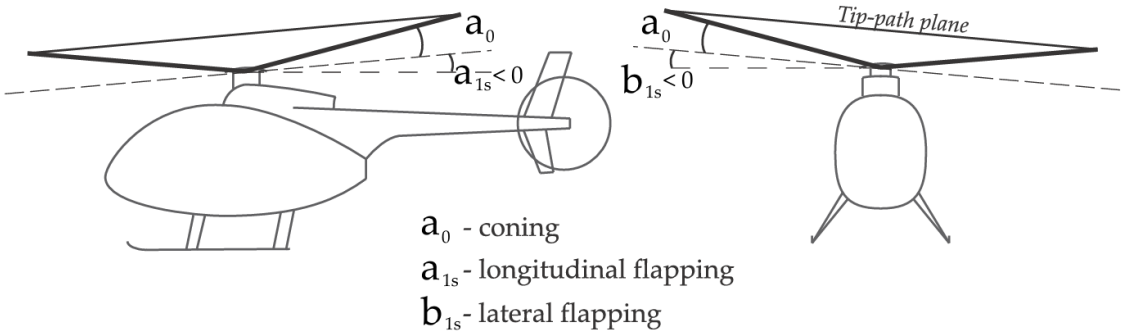

Figure 2: Visualization of flapping angles in the tip-path-plane approximation.

in which λ is the inflow ratio, μ is the advance ratio, w_H is the relative wind velocity on the rotor, C_T is the thrust coefficient. Rotor thrust is given by:

$$T = \frac{1}{2} N_b \rho a c R (\Omega R)^2 \left(\frac{\lambda}{2} + \theta_0 \left(\frac{1}{3} + \frac{\mu^2}{2} \right) + \theta_t \left(\frac{1}{4} + \frac{\mu^2}{4} \right) \right) \tag{10}$$

in which N_b is the number of blades, a is the blade lift slope, c is the chord, θ_0 is the collective or blade root pitch and θ_t is the blade twist. The two equations are coupled, resulting in a non-linear problem and thus they are solved iteratively at each time-step by means of a Newton-Raphson algorithm.

The rotor H-force and torque are given by:

$$H_w = \frac{N_b}{2} \rho \, a \, c \, R \, (\Omega R)^2 \left(\frac{\delta \mu}{2a} - \frac{1}{4} \theta_0 (2\lambda\mu) - \frac{\theta_t}{4} (\mu\lambda) + \frac{\mu}{4} a_0^2 \right) \tag{11}$$

$$Q = k_{\text{ind}} \frac{N_b}{2} \rho \, a \, c \, R^2 \, (\Omega R)^2 \left(\frac{\delta}{k_{\text{ind}} (4a)} (1 + \mu^2) - \theta_0 \frac{\lambda}{3} - \frac{\theta_t \lambda}{4} - \frac{1}{2} \lambda^2 \right) \tag{12}$$

in which $\delta = C_{d_o} + C_{d_1} \overline{\alpha} + C_{d_2} \overline{\alpha}^2$ is the profile drag coefficient calculated using the average angle of attack.

Mind that all variables are in the hub-wind axis and forces and moments are rotated afterwards in hub-body considering the sideslip angle of the rotor. Also, the effect of external wind on the tail rotor was neglected in the current work.

2.1.4 Flapping

The flapping motion of helicopter rotor blades is a highly damped out of plane oscillation in resonance with the rotor angular rate (see Padfield[4] and Prouty[5]). It can be modeled by a first order Fourier series employing the *tip-path-plane* approximation, moreover we can reasonably approximate its dynamics as a first order system with time constant calculated as:

$$T_{flap} = \frac{16}{\gamma \Omega} \tag{13}$$

where γ is the Lock number. For a teetering helicopter, we can treat the coning angle a_0 as a preset constant. Then the steady state values of flapping angles are given by Prouty[5] as:

$$a_{1w} = \frac{\frac{8}{3}\theta_0\mu + 2\theta_t\mu - B_{1w}\left(1 + \frac{3}{2}\mu^2\right) - 2\mu\lambda - \frac{16}{\gamma}\frac{q_w}{\Omega} + \frac{p_w}{\Omega}}{1 - \frac{\mu^2}{2}} \tag{14}$$

$$b_{1w} = A_{1w} + \frac{\frac{4}{3}\mu a_0 - \frac{16}{\gamma}\frac{p_w}{\Omega} - \frac{q_w}{\Omega}}{1 + \frac{\mu^2}{2}} \tag{15}$$

in which both the flapping and feathering (cyclic pitch) inputs are in hub-wind axis. We see here the contribution of external wind through the advance ratio μ and of the body angular rates p and q, due to gyroscopic effects. The back rotation to hub-body axis is obtained through:

$$\begin{aligned} a_{1s} &= a_{1w}\cos\beta_w + b_{1w}\sin\beta_w \\ b_{1s} &= -a_{1w}\sin\beta_w + b_{1w}\cos\beta_w \end{aligned}$$

in which β_w is the rotor sideslip angle.

2.1.5 Fuselage drag

The fuselage aerodynamic forces are reduced to the drag alone, which is modeled through its equivalent flat plate area in the frontal, lateral and vertical directions:

$$\vec{D}_f = -\frac{1}{2}\rho\left([A_x, A_y, A_z]^t \odot \vec{v_B}\right)||\vec{v_B}|| \tag{16}$$

with $\odot$ indicating element-wise multiplication.

2.1.6 Pilot controls

The helicopter is controlled through cyclic and collective pitch inputs:

- collective pitch $\theta_{0_{mr}}$: controls the main rotor thrust by adjusting the pitch of all blades equally around the azimuth.
- lateral and longitudinal cyclic pitch A_{1s}, B_{1s}: controls the tilting of the rotor disc and thus of the thrust vector inducing pitching and yawing moments.
- tail rotor pitch ($\theta_{0_{tr}}$): controls yaw motion by regulating tail rotor thrust.

The vertical channel is controlled solely via the collective pitch, while longitudinal and lateral angular rates are regulated through cyclic pitch-induced flapping. The control authority varies with the collective setting. The yaw is controlled by the pedals which are connected to the tail rotor collective pitch linkage. The controls are normalized between $[-1, 1]$ using the ranges specified in appendix A, and in normalized form are indicated as:

$$\vec{u} = [\delta_A, \delta_B, \delta_C, \delta_P]^t \tag{17}$$

2.2 Linearized model

If we analytically linearize the model around the hover condition, neglecting the contribution of some smaller forces, we get the affine linear system describing the attitude dynamics:[3]

$$\dot{\vec{x}} = \vec{f} + \underline{\underline{B}}\vec{u} + \vec{\Delta}(\vec{x}, \vec{u}) \tag{18}$$

$$\vec{f} = \begin{bmatrix} 0 \\ 0 \\ \frac{Q_M}{I_{zz}} \end{bmatrix} \tag{19}$$

$$\underline{\underline{B}} = \begin{bmatrix} \frac{l_{z_{mr}} T_M}{I_{xx}} & 0 & 0 \\ 0 & -\frac{l_{z_{mr}} T_M}{I_{yy}} & 0 \\ 0 & 0 & -\frac{l_{x_{tr}} k_{tr}}{I_{zz}} \end{bmatrix} \tag{20}$$

$$\tag{21}$$

with $\vec{x} = [p, q, r]^t$, $\vec{u} = [A_{1s}, B_{1s}, \theta_{o_{tr}}]$. We have assumed here that the main rotor collective, and thus thrust and torque, stay constant and equal to the hover trim value. The relation between tail rotor thrust and pitch input is linearized through the constant of proportionality k_{tr}. It must be noted that another matrix is needed to transform the dimensional inputs into the adimensionalized ones, in order to be consistent with the complete model and correctly design the control law. Its contribution is considered to be included in $\underline{\underline{B}}$ in what follows.

2.3 FEL Controller design

The proposed controller governs the attitude of the aircraft by commanding the cyclic and pedal inputs. It is an angular rate controller and receives a set point of attitude angles, which is transformed into an angular rate set point by a proportional gain. It is aided by a neural network which estimates the model uncertainties and disturbances, which ensures that all signals in the closed-loop system remain bounded.

Feedback Error Learning employs a control law based on a nominal model of the system, which in our case is given by the linear attitude dynamics in hover of equation 18.

Following the work of Castaldi,[1] we can define the desired trajectory as $\vec{x}_{sp}$ and the tracking error as $e = \vec{x} - \vec{x}_{sp}$. Then we introduce the filtered error s:

$$s = e + \underline{\underline{\lambda}} \int_0^t e dt \tag{22}$$

differentiating we obtain:

$$\dot{s} = \dot{\vec{x}} - \dot{\vec{x}}_{sp} + \underline{\underline{\lambda}} e = \vec{f} + \underline{\underline{B}}\vec{u} + \vec{\Delta}(\vec{x}, \vec{u}) - \dot{\vec{x}}_{sp} + \underline{\underline{\lambda}} e$$

and the control command can then be defined as:

$$\vec{u} = \underline{\underline{B}}^{-1} \left(-\vec{f} - \vec{\Delta}(\vec{x}, \vec{u}) + \dot{x}_{sp} - \underline{\underline{\lambda}} e - \underline{\underline{k}} s \right), \tag{23}$$

where $\underline{\underline{\lambda}}$ and $\underline{\underline{k}}$ are diagonal, positive-definite matrices. However, the vector $\vec{\Delta}$ is unknown. Thus, it is approximated by the radial basis function neural network as:

$$\hat{\Delta} = \underline{\underline{W}}^t \vec{\mu}(\vec{X})$$

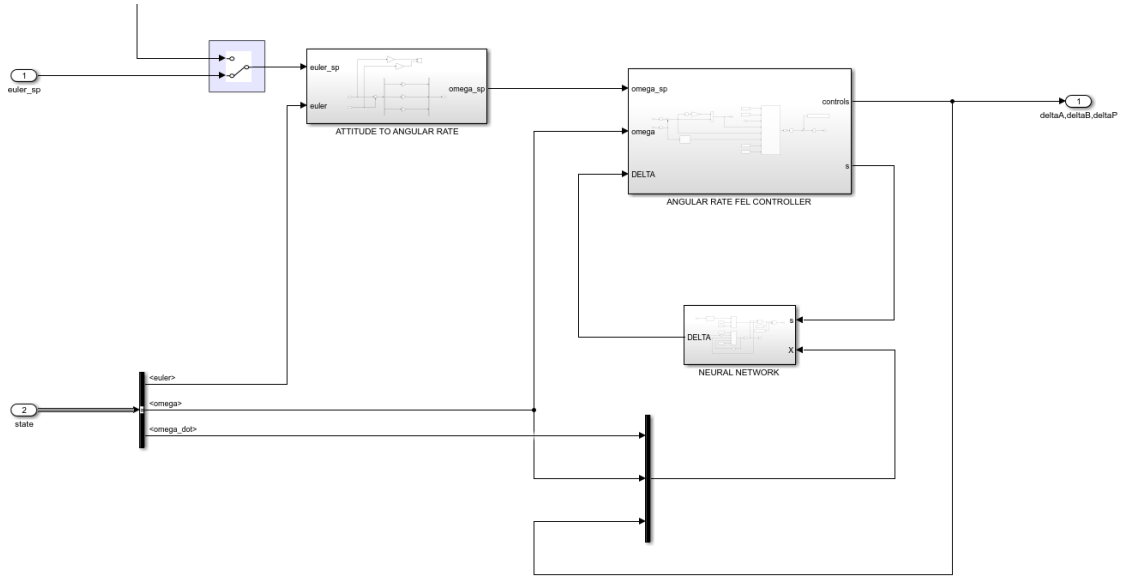

Figure 3: Structure of the RBFNN-FEL controller.

where $\vec{\mu}$ represents the vector of basis functions (corresponding to hidden layers of the NN) and $\underline{\underline{W}}$ indicates the matrix of unknown weights that should be identified. The activation functions are Gaussian shaped and $\vec{\mu}$ is calculated as:

$$\mu_i(\vec{X}) = exp\left(-\frac{(\vec{X} - x_{o_i})^t \cdot (\vec{X} - x_{o_i})}{2\sigma_i^2}\right) \frac{1}{\sqrt{2\pi\sigma_i^2}} \tag{24}$$

in which the input to the neural network is $\vec{X} = [\dot{\vec{x}}, \vec{x}, \vec{u}]$, and $\vec{x}_o$ and $\vec{\sigma}$ are the vectors of centers and widths for the neurons. The online learning of the NN is based on a gradient descent algorithm aimed at zeroing the error, which results in the following update rule for the weights:

$$\dot{\underline{\underline{W}}} = \eta \left(\vec{\mu}(\vec{X}) \cdot s^t - \sigma \underline{\underline{W_0}}\right) \tag{25}$$

in which $\eta > 0$ is the learning rate, and $\sigma > 0$ acts as a relaxation factor, slowing the update when the weights get too large by multiplying their value at the previous step. This procedure helps to reach convergence of matrix $\underline{\underline{W}}$ in absence of persistent excitation and is regarded as *sigma-modification*.

Angular Rate FEL Controller Parameters	
λ	$\texttt{diag}(0.08, 0.05, 1.5)$
k	$\texttt{diag}(3.7, 5, 10)$
RBF Neural Network Parameters	
number of neurons	15
$\vec{x}_o$ (centers)	$\texttt{linspace}(-1, 1, 15)^t$
$\vec{\sigma}$ (widths)	$\texttt{linspace}(1.2, 4.2, 15)^t$
$\underline{\underline{W_o}}$ (initial weights)	$\texttt{zeros}(\texttt{neurons}, 3)$
η (learning rate)	1

Table 1: RBFNN-FEL controller parameters.

3 Results

The helicopter dynamic model and the controller were implemented in a MATLAB Simulink environment. We show here the results of various test scenarios. The controller parameters are listed in table 1.

3.1 Comparison between linear and non-linear model

The design and tuning of the FEL controller were performed on the linearized attitude model of the aircraft, in which case it does not need any correction since it is exactly predicted by the system model implemented in the controller. Then the controller was applied to the non-liner system, without any modification. In figure 4 we can see the closed loop response to an attitude set point step input for both the linear and non-linear model, with and without the correction from the neural network. We can see that the FEL controller alone does not perform well when applied to the complete model: the response is slower and with a large steady state error. When turning on the neural network the response is greatly improved, which demonstrates that it is capable to estimate the previously unmodeled dynamics and non-linearities of the system.

3.2 Attitude setpoint tracking under wind shear

We now introduce a disturbance in the form of wind shear. We remind that effects of the wind are considered in the dynamic model as fuselage and rotor drag, variation in rotor thrust and induced flapping. Wind shear was modeled as:

$$W = \begin{bmatrix} 5\sin\left(\frac{\pi}{4}t + \frac{\pi}{4}\right) \\ 5\sin\left(\frac{\pi}{4}t + \frac{\pi}{4}\right) \\ 0 \end{bmatrix} \tag{26}$$

where wind velocity is expressed in m/s in the local vertical frame.

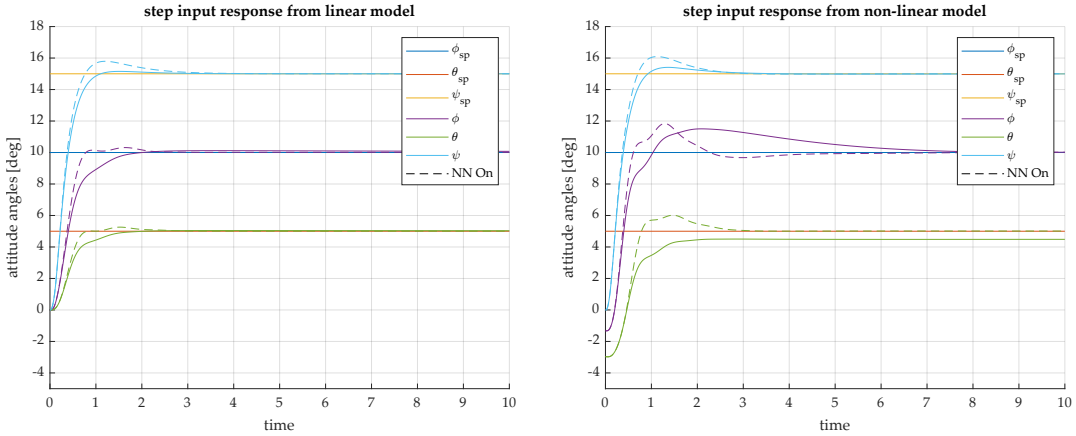

(a) Linearized attitude dynamics model

(b) Complete non-linear 6DoF helicopter model

Figure 4: Performance of the RBFNN-FEL controller with a step input setpoint of attitude angles in a hover condition. The dotted lines correspond with the activation of the neural network.

First we test the attitude response of the system when given a sinusoidal angle setpoint, expressed as:

$$\begin{aligned} \phi_{\text{sp}} &= 10\cos\left(\frac{2\pi}{15}t - \frac{\pi}{3}\right) \\ \theta_{\text{sp}} &= 5\cos\left(\frac{2\pi}{15}t - \frac{\pi}{3}\right) \\ \psi_{\text{sp}} &= 0 \end{aligned} \tag{27}$$

The result is visible in figure 5. We can see how the neural network manages to improve the tracking despite the disturbances. When examining the results we must keep in mind that the inertia of the helicopter around the pitch axis is much higher than around the roll axis.

3.3 Trajectory tracking under wind shear

To further evaluate the neural adaptive attitude controller, an outer loop for position control was added using a basic PID structure. This loop manages the vertical channel by adjusting the collective input and sets the desired attitude reference for the RBFNN-FEL controller to track, which then handles the cyclic pitch and pedal inputs. The test trajectory is a climbing turn with a radius of 8m, a turn rate of 12deg/s, and a constant rate of climb of 787,4ft/s (4m/s) given by:

$$\begin{aligned} x_{\text{sp}} &= 8\cos\left(\frac{2\pi}{30}t\right) - 8, \\ y_{\text{sp}} &= 8\sin\left(\frac{2\pi}{30}t\right). \end{aligned} \tag{28}$$

The result is visible in figure 6. The action of the neural network enhances the accuracy, although its influence on the position control is limited since it is applied only to the attitude controller.

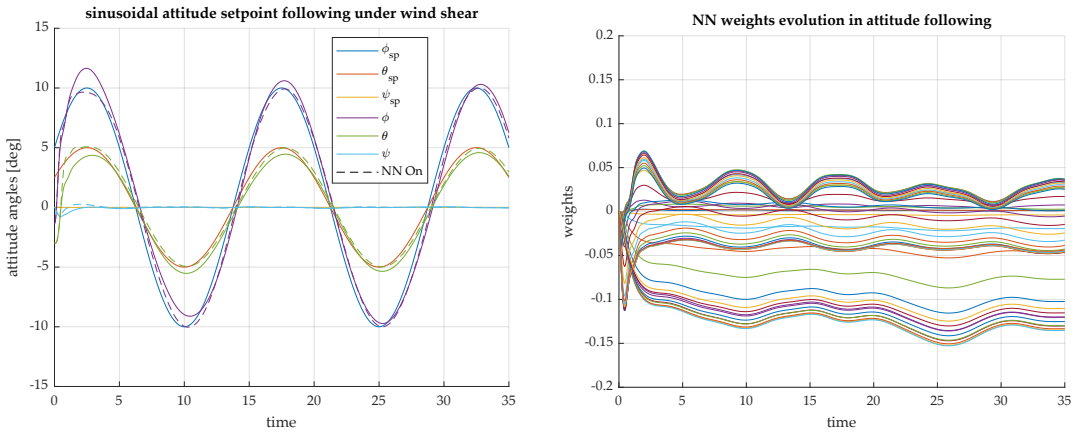

(a) Sinusoidal attitude setpoint following under wind shear

(b) Evolution in time of the neural network weights

Figure 5: Performance of the RBFNN-FEL controller when applied to the non-linear 6DoF helicopter model to follow a sinusoidal setpoint of attitude angles, under wind gusts disturbances. The dotted lines correspond with the activation of the neural network. The evolution of the weights is reported to show the online learning of the network.

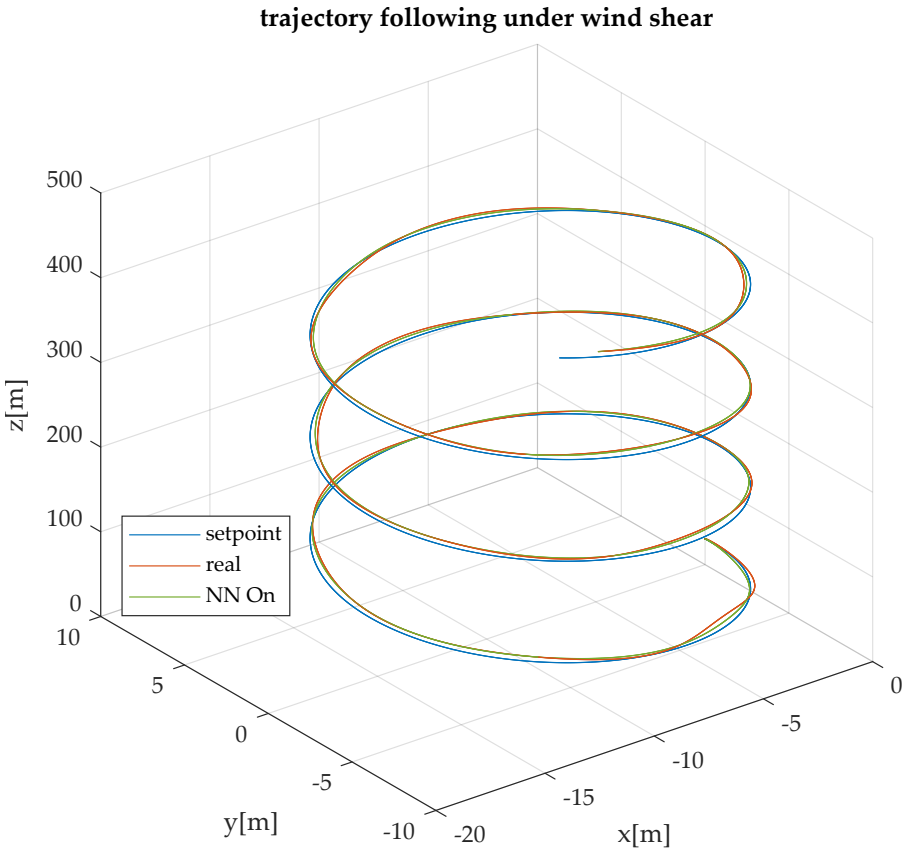

Figure 6: Trajectory following under wind shear in a climbing turn maneuver.

4 Conclusions

This project has demonstrated the effectiveness of a Feedback Error Learning (FEL) controller enhanced by a Radial Basis Function Neural Network (RBF-NN) for the attitude control of a teetering rotor helicopter. The FEL controller, based on a linearized model of the helicopter's attitude dynamics, was able to achieve satisfactory performance in hover conditions. However, when applied to the non-linear 6DoF model, the controller exhibited significant steady-state errors and slower response times, highlighting the limitations of relying solely on a linearized model.

The integration of the RBF-NN into the control architecture proved to be a crucial enhancement. The neural network successfully estimated and compensated for the unmodeled dynamics and external disturbances, significantly improving the controller's performance. This was particularly evident in the presence of wind shear, where the RBF-NN enabled the helicopter to maintain accurate attitude tracking despite the challenging conditions. The online learning capability of the RBF-NN, driven by a gradient descent algorithm, allowed the system to adapt in real-time, ensuring robust performance across various flight scenarios.

The simulation results also demonstrated the controller's ability to handle more complex maneuvers, such as trajectory tracking during a climbing turn. While the RBF-NN's influence was limited to the attitude control loop, some improvement in the overall result was obtained. It would be interesting to implement an adaptive controller in the guidance loop as well, and test if additional improvement in trajectory tracking of aggressive maneuvers can be achieved.

A Helicopter model parameters

Inertial Parameters		
`m`	8000	Take-off mass [Lbs]
`I_xx`	2700	Moment of inertia about x-axis [slug $\cdot$ ft^2]
`I_yy`	12800	Moment of inertia about y-axis [slug $\cdot$ ft^2]
`I_zz`	10800	Moment of inertia about z-axis [slug $\cdot$ ft^2]
`I_xz`	950	Product of inertia [slug $\cdot$ ft^2]
Environmental Conditions		
`rho`	1.225	Air density at sea level [kg/m^3]
`g`	9.81	Gravity acceleration [m/s^2]
Controls Input Range		
`lon_cyc_range`	$[-15, 15]$	Longitudinal cyclic range [deg] (positive aft)
`lat_cyc_range`	$[-15, 15]$	Lateral cyclic range [deg] (positive right)
`mr_coll_range`	$[7.5, 25]$	Main rotor collective range [deg] (positive up)
`tr_coll_range`	$[-20, 20]$	Tail rotor collective range [deg] (positive right)
Main Rotor Parameters		
`OMEGA`	314	Angular speed [rpm]
`BLADES`	2	Number of blades
`ROTOR`	22	Rotor radius [ft]
`CHORD`	2.25	Mean aerodynamic chord [ft]
`ASLOPE`	6.28	Blade lift curve slope [1/rad]
`AOP`	2.75	Precone angle [deg]
`GAMMA`	5.216	Lock number
`THETT`	-10	Blade twist [deg]
`T_flap`	0.0933	Time constant for flapping [s] from eq.13
`CD_mr`	$[0.009, 0, 0.3]$	Drag coefficients [CD0, CD1, CD2]
`L_mr`	$[-0.1, 0, -2.03]^t$	Position relative to CG [m]
Tail Rotor Parameters		
`AOPTR`	0	Precone angle [rad]
Ω_{TR}	1608.5	Angular speed [rpm]

Continues in the next page

Follows from previous page

BLADESTR	2	Number of blades
ROTORTR	4.25	Rotor radius [ft]
CHORDTR	0.7	Mean aerodynamic chord [ft]
ASLOPETR	6.28	Blade lift curve slope [1/rad]
GAMMATR	2.23	Lock number
THETTTR	0	Blade twist [deg]
CD_tr	$[0.009, 0, 0.3]$	Drag coefficients [CD0, CD1, CD2]
L_tr	$[-8.25, 0, -1.15]^t$	Position relative to CG [m]
Fuselage Parameters		
L_fus	$[-0.1, 0, 0.48]^t$	Position relative to CG [m]
Ax	5.5	Equivalent drag area in x-direction [ft^2]
Ay	156.1	Equivalent drag area in y-direction [ft^2]
Az	84.7	Equivalent drag area in z-direction [ft^2]

Concludes from previous page

References

[1] S.A. Emami, P. Castaldi, A. Banazadeh, "Neural network-based flight control systems: Present and future", *Annual Reviews in Control*, 2022

[2] S. Shen, J.Xu, "Adaptive neural network-based active disturbance rejection flight control of an unmanned helicopter", *Aerospace Science and Technology*, 2021

[3] B. Godbolt, " Experimental Validation of a Helicopter Autopilot Design using Model-Based PID Control", *Journal of Intelligent Robot Systems*, 2013

[4] G.D. Padfield, "Helicopter flight dynamics"

[5] R. Prouty, "Helicopter performance, stability and control"

[6] P.D. Talbot, "A mathematical model for a single main rotor helicopter for piloted simulations", *NASA TM-84281*, 1982